LASER MANIPULATION OF RYDBERG QUANTUM STATES

Dr. Aigars Ekers, MSc. Artūrs Ciniņš, MSc. Mārtiņš Brūvelis

Activity "Laser manipulation of Rydberg quantum states" of the research project was carried out at Molecular beam laboratory of Laser Centre of the University of Latvia. Research in the area of quantum manipulation of highly excited quantum states was carried out. Theoretical and experimental studies of new population control methods and population dynamics of Rydberg states were performed. A new mathematical model accurately describing formation of residual Doppler profile of geometrically cooled supersonic atomic/molecular beams for arbitrary collimating aperture was developed within the research project. Studies of dressed state formation in systems with hyperfine structure have led to development of a theoretical model which describes formation of hyperfine structure of laser-field dressed atomic states. Investigation of population dynamics of Rydberg states has allowed development of a novel technique for measuring radiative constants of Rydberg states in atoms. In addition, several improvements to technical equipment of the laboratory were made within the research project.

1. Particularities of residual Doppler profile in geometrically cooled supersonic atomic/molecular beams

Limiting factor in majority of measurements in atomic and molecular spectroscopy is the Doppler effect. Effective photon energy shifts caused by atomic (molecular) thermal motion gives rise to inhomogeneous broadening of spectral lines. Confinement and cooling of atomic/molecular media is imperative in the field of high resolution spectroscopy. One of the widely used cooling techniques is supersonic expansion and reduction of thermal movement in two dimensions by means of geometrical cooling of supersonic beams. Experimental studies and development of coherent manipulation techniques of Rydberg states all employ this cooling technique to obtain low temperature atomic beams. Experimental studies involve selection of optimal experimental setup. In addition, experimental data can be interpreted properly only if all non-negligible effects which influence spectral linewidth and lineshape of quantum particles are taken into account. Such effects include the previously studied transit time broadening of spectral line due to finite atom – laser field interaction time. Studies of effect of geometrical properties of supersonic beam on spectral lineshape function were carried out within the current research project.

At the region close to the beam source (nozzle) intense non-adiabatic inter-particle collisions take place. Therefore thermodynamical equilibrium between velocities in directions parallel and perpendicular to the beam axis is not maintained. Rapid expansion of the particle cloud leads to quickly decaying rate of collisions therefore energy exchange between the two velocity components becomes ineffective until at a certain distance from the nozzle collision rate becomes negligible. The distance from the nozzle is called the freezing point. Beyond the freezing point the radial velocity component changes no more thus becoming "frozen". Due to nonzero value of velocity in the direction perpendicular to the beam axis, particles move away from the beam axis. The average velocity in the perpendicular direction per unit area continues to decrease as the cloud expands while velocity in the radial direction remains

constant due to low collision rate. Therefore temperatures corresponding to parallel and perpendicular velocity directions need to be described separately. In addition, by using several skimmers and a final beam collimating aperture, particles with large perpendicular velocity component do not pass through collimating aperture and thus only particles with slow perpendicular velocity become part of a collimated beam. This physical effect is usually referred to as geometrical cooling.

Physical aspects of a molecular supersonic beam machine suggest that the following approximations are applicable:

1. Particles (atoms or molecules) are emitted isotropically from the nozzle S' due to a small solid angle of a well collimated beam;
2. Number of interatomic (intermolecular) collisions in the space between the nozzle and the collimating aperture S is negligible;

Coordinate system is chosen such that direction of laser excitation of the atomic/molecular beam coincides with the e_x axis.

In this case the Doppler broadening of a spectral lineshape for arbitrarily shaped collimating aperture is expressed as:

$$P_D(\nu) = P(\Delta\nu) = \frac{1}{S' \times S} \iint_{S'} dy'dx' \iint_{S} dydx \int_0^{\infty} dvF(v) \times \delta(\Delta\nu - \frac{(x-x')v}{L\lambda})$$

Here Δv is detuning of laser frequency from atomic transition resonance, $\iint_{S'} dx'dy'$ - integration over the area of nozzle, $\iint_{S} dxdy$ - integration over the area of collimating aperture, L - distance between nozzle and collimating aperture, λ - wavelength of the selected atomic transition, v - absolute velocity of an atom/molecule inside the beam, $F(v)$ - velocity distribution function for atoms/molecules inside the beam.

Calculations were performed for two special cases: if a circular or quadratic collimating aperture is used. The integral expression in the case of circular aperture is:

$$P_{circ} = \int_{-r_1}^{r_1} \int_{-\sqrt{r_1^2-(x')^2}}^{\sqrt{r_1^2-(x')^2}} \int_{-r_2}^{r_2} \int_{-\sqrt{r_2^2-(x)^2}}^{\sqrt{r_2^2-(x)^2}} \int_{-\infty}^{\infty} F(v) \times \delta\left(\nu - \frac{(x-x')^2}{L\lambda}\right) dvdydxdy'dx'$$

And for quadratic collimating aperture:

$$P_{kvadr}(\nu) = \int_{-r_1}^{r_1} \int_{-\sqrt{r_1^2-(x')^2}}^{\sqrt{r_1^2-(x')^2}} \int_{-r_2}^{r_2} \int_{-r_2}^{r_2} \int_{-\infty}^{\infty} F(v) \times \delta\left(\nu - \frac{(x-x')^2}{L\lambda}\right) dvdydxdy'dx'$$

Solving these expressions numerically requires large amounts of computational power. In addition, at small values of $\Delta\nu$ the result of calculations is disturbed by finite precision of the selected numerical method (fig 1). Increase of the precision leads to even more computational power required for the calculation. Therefore analytical solutions of the expressions were searched for.

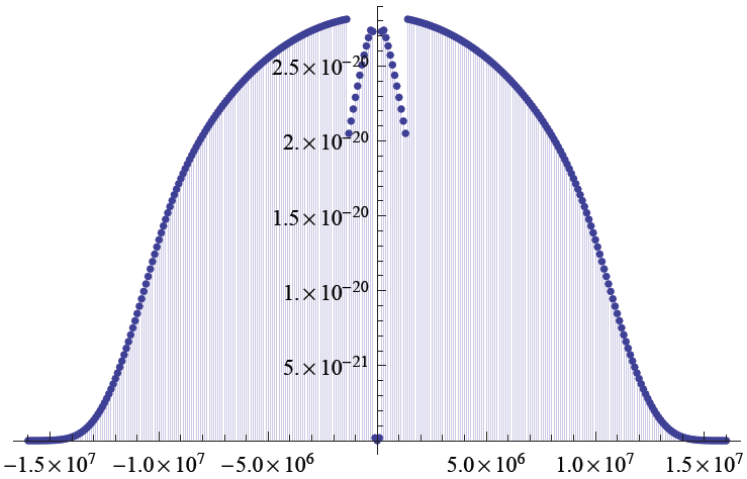

Fig 1. Numerical convolution of Doppler and Lorentz profiles provides incorrect solution at small values of $\Delta\nu$.

Assuming infinitely small nozzle area and assuming that velocity distribution function $F(v)$ is the Dirac delta function, expression for Doppler profile kernel was obtained for circular collimating aperture:

$$\tilde{P}(\Delta\nu) = \frac{2}{\Delta\nu_K \pi}\sqrt{1 - \frac{\Delta\nu^2}{\Delta\nu_K^2}}$$

Here $\Delta\nu_k$ is the characteristic width of the residual Doppler profile. Comparison with numerical simulation results reveals noticeable differences from both numerical simulations for circular and quadratic collimating apertures (fig 2).

In calculations natural linewidths of all transitions and spectral linewidth of laser radiation must be taken into account. Both profiles are described by Lorentzian functions, therefore actual lineshape of residual Doppler profile must be a convolution of a Doppler type function and a Lorentzian function,

$$J_L(\nu) = \frac{2\Delta\nu_l}{\pi \times \Delta\nu_l^2 + 4\pi \times \nu^2}$$

Search for an analytical expression is again motivated by the fact that numerical calculation of convolution of Doppler and Lorentzian lineshapes (fig 3) requires larege amounts of computational power. Approximate analytical solution to convolution of Doppler profile kernel and Lorentz lineshape was found to be:

$$J_L(\nu) = \frac{\sqrt{2}}{\pi}\sqrt{\sqrt{(x_r^2 - a^2 - 1)^2 + 4x_r^2 a^2} + 1 - x_r^2 + a^2} - \frac{2a}{\pi}$$

Here $a = \frac{\Delta\nu_{laser}}{2\Delta\nu_k}$, $x_r = \frac{\Delta\nu_{laser}}{\Delta\nu_k}$, $\Delta\nu_{laser} = \nu_{resonance} - \nu_{laser}$. Analytical expression obtained by this method presents a good match with the numerical simulation data (fig 4).

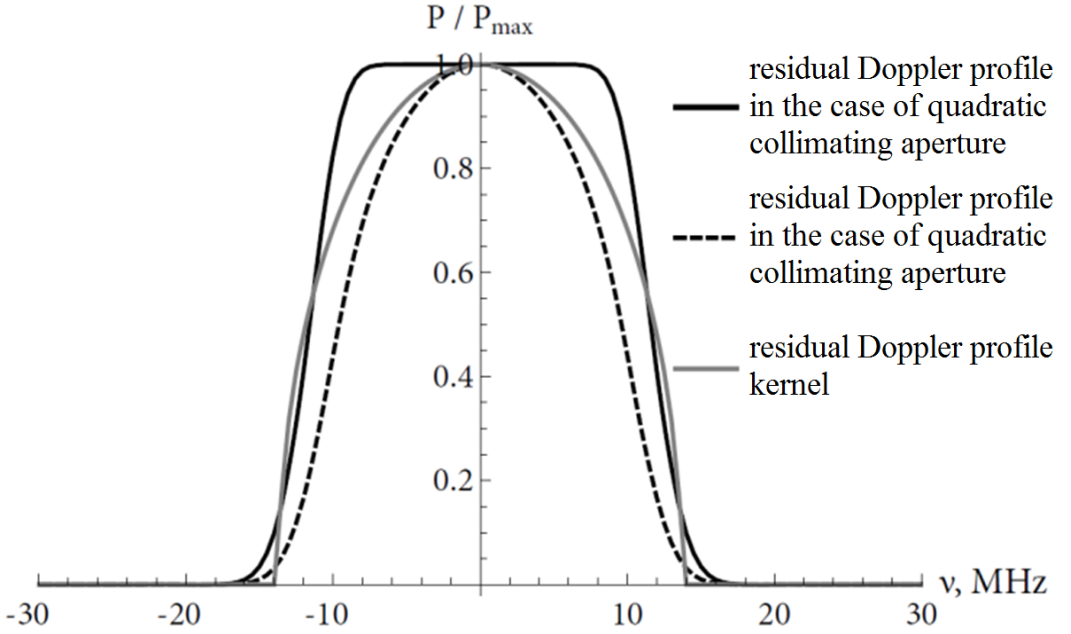

Fig 2. Comparison of numerical simulations of residual Doppler profiles for circular and square collimating apertures and the so-called Doppler profile kernel. Typical parameters of the experimental device are used in the simulations.

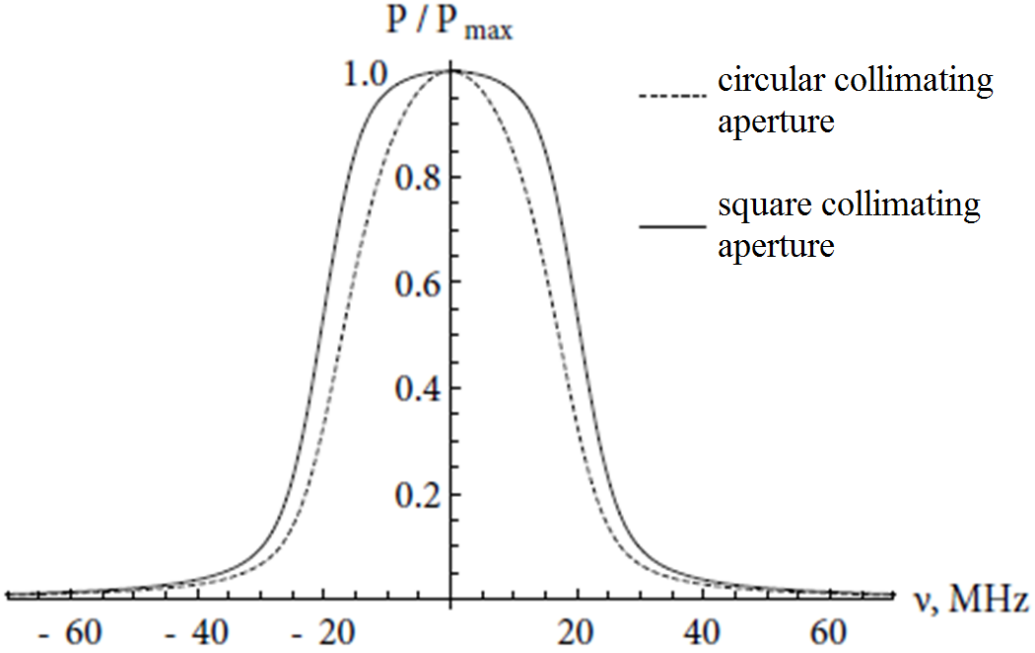

Fig 3. Numerical convolution of Doppler and Lorentz profiles. Typical parameters of the experimental device are used in the simulations.

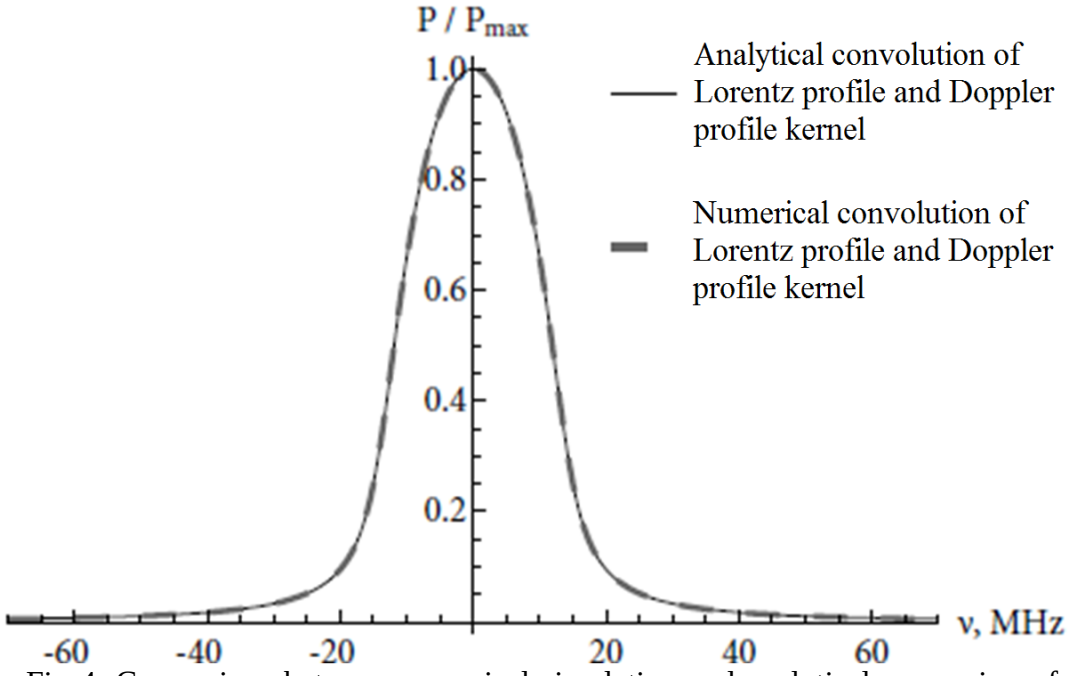

Fig 4. Comparison between numerical simulation and analytical expression of Doppler profile and Lorentz profile convolution. Typical parameters of the experimental device are used in the simulations.

The main advantage of analytical expression for Doppler and Lorentz lineshape convolution is the chance to perform quick calculations of the profile shape. Two main differences from numerical solution are expected due to finite size of the nozzle:

1. Middle part of the numerical convolution is more narrow than the analytical solution (due to analogous difference between Doppler profile and Doppler profile kernel);
2. Wings of the analytical solution are less pronounced due to the constant velocity assumption used in evaluating expression for Doppler kernel.

Series of experimental measurements were performed in order to confirm predictions of the theoretical model for residual Doppler profile lineshape. Schematic view of experimental setup is depicted in fig 5. The experimental setup consists of two laser systems: a dye ring laser *Coherent 699-21* and a frequency-doubled high power system *Toptica TA-SGH110*. Typical linewidths of laser radiation are accordingly *1MHz* and *2MHz*.

Analytical solutions were obtained assuming infinitely small natural linewidth of atomic spectral lines. Therefore excitation scheme must involve a long lived highly excited energy level. Two excitation schemes of sodium atoms were tested: $3S_{1/2} \rightarrow 3P_{1/2} \rightarrow 8S_{1/2}$ and $3S_{1/2} \rightarrow 3P_{1/2} \rightarrow 7D_{3/2}$, with lifetimes of the final state accordingly *405,94ns* and *312,43ns*.

Preliminary numerical calculations were performed at very low resolution to increase calculation speed (fig 6). The analytical model developed within this study allows performing numerical simulations at very high spatial resolutions reducing amount of computational resources required at the same time. Analysis of experimental data has revealed that experimental data points coincide best with the predictions of residual Doppler effect model combined with effect of finite natural linewidth of spectral lines.

On some occasions experimental data coincide best with a Gaussian function (fig_7) since the effect described by the theoretical model is small compared to other

broadening effects in the case of circular collimating aperture. Therefore measurements for other shapes of collimating aperture are required to verify the model experimentally. Experimental measurement of residual Doppler profiles in the case of square collimating aperture is currently being prepared at the Molecular beam laboratory. In this case residual Doppler profile is predicted to have less pronounced wings and a broad maximum (fig 2).

The study has led to development of a mathematical model which describes influence of shape of beam collimating aperture to spectral lineshape of residual Doppler profile in geometrically cooled supersonic atomic/molecular beams. Methods for exact calculation and approximate solutions of residual Doppler profile lineshape in cases of circular and square collimating aperture were developed. Within the research data of more than 140 residual Doppler profile measurements were gathered for two-photon excitation to excited states $8S_{1/2}$ and $7D_{3/2}$ of sodium. Experimental studies have led to a conclusion that hyperfine splitting of $8S_{1/2}$ state of sodium is comparable to width of residual Doppler profile, therefore approximate methods provide incorrect estimates of residual Doppler profile lineshape. At large laser field power values formation of residual Doppler profile of $7D_{3/2}$ state is dominated by broadening processes which are best described by the Gaussian function. However, at reduced laser powers residual Doppler profile is better described by the calculated analytical convolution of Doppler and Lorentz profiles. Due to the fact that residual Doppler profile lineshape depends both on shape of the nozzle and shape of the collimating aperture, it is impossible to obtain a general solution for the residual lineshape. Before this study description of residual Doppler profile lineshape was limited to estimate of profile linewidth using Gaussian or Voigt type functions to fit experimental data. This approach yields invalid results when influence of Doppler broadening becomes comparable to other lineshape broadening effects or to natural linewidth of the transition. For example, quadratic collimating aperture leads to peculiar lineshape profile, which differs significantly from Gaussian and Voigt type functions. Results of this study provide opportunity to develop novel experimental applications of geometrically cooled atomic beams. For example, it is possible to employ the developed model in calculating spectral linewidth of laser radiation at the time of an experimental measurement. This method is based on the fact that experimentally measured profile is actually a convolution of residual Doppler profile and laser radiation lineshape. By performing reverse operation of convolution spectral linewidth and even lineshape of laser radiation is obtained. Results of this study are relevant to supersonic beams only since otherwise assumption of no collisions in the beam is violated.

Basic ideas of the study were presented at seminar of the doctoral school “Atomāro un nepārtrauktas vides fizikālo procesu pētīšanas, modelēšanas un matemātisko metožu pilnveidošanas skola” in oral presentation “Residual Doppler profile in supersonic molecular beam”. Results of the research were presented at the conference *EGAS 43* in Fribourg (Switzerland) [1] and at the *21st International Conference on Spectral Line Shapes* in Saint Petersburg (Russia) [2]. Theory part of unpublished scientific paper on the subject of the research was prepared within the research project [3].

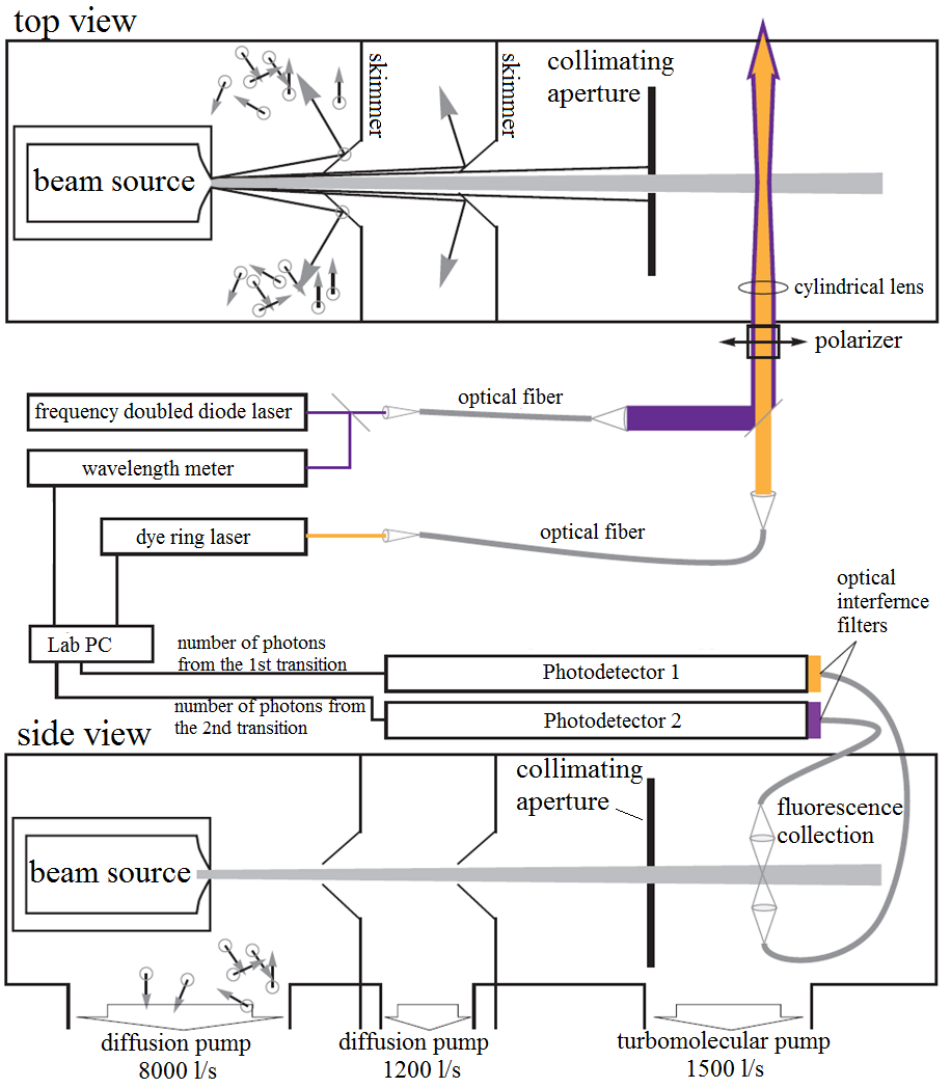

Fig 5. Experimental setup for residual Doppler profile measurement in supersonic atomic/molecular beams. Differential vacuum pumping system allows to achieve lower pressure in the reaction chamber. Spontaneously emitted radiation is collected using lenses and optical fibers.

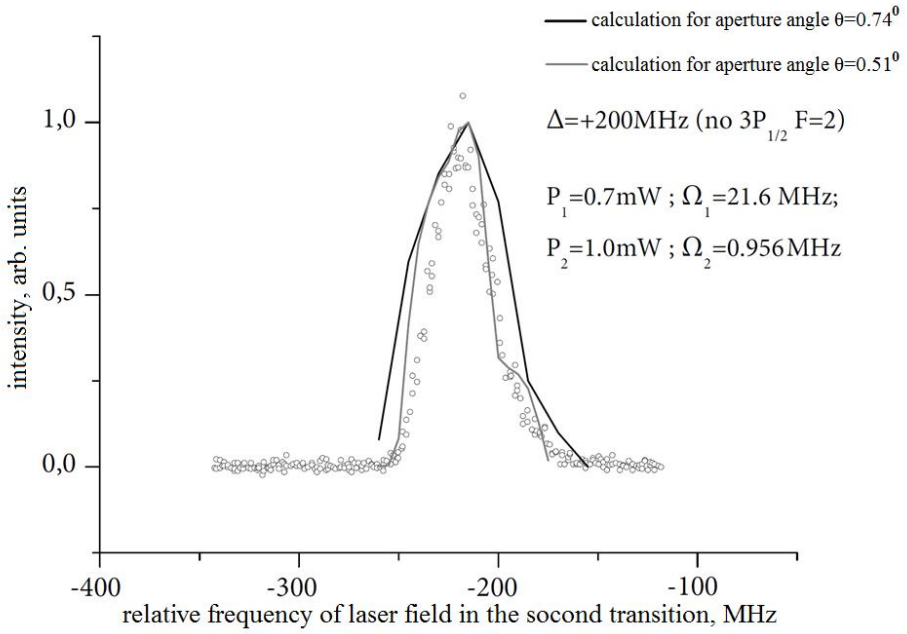

Fig 6. Residual Doppler profile of transition $3S_{1/2} \rightarrow 3P_{1/2} \rightarrow 8S_{1/2}$ in sodium. Two lasers P1 and P2 induce transitions accordingly $3S_{1/2} \rightarrow 3P_{1/2}$ and $3P_{1/2} \rightarrow 8S_{1/2}$. Detuning of P1 is represented by Δ.

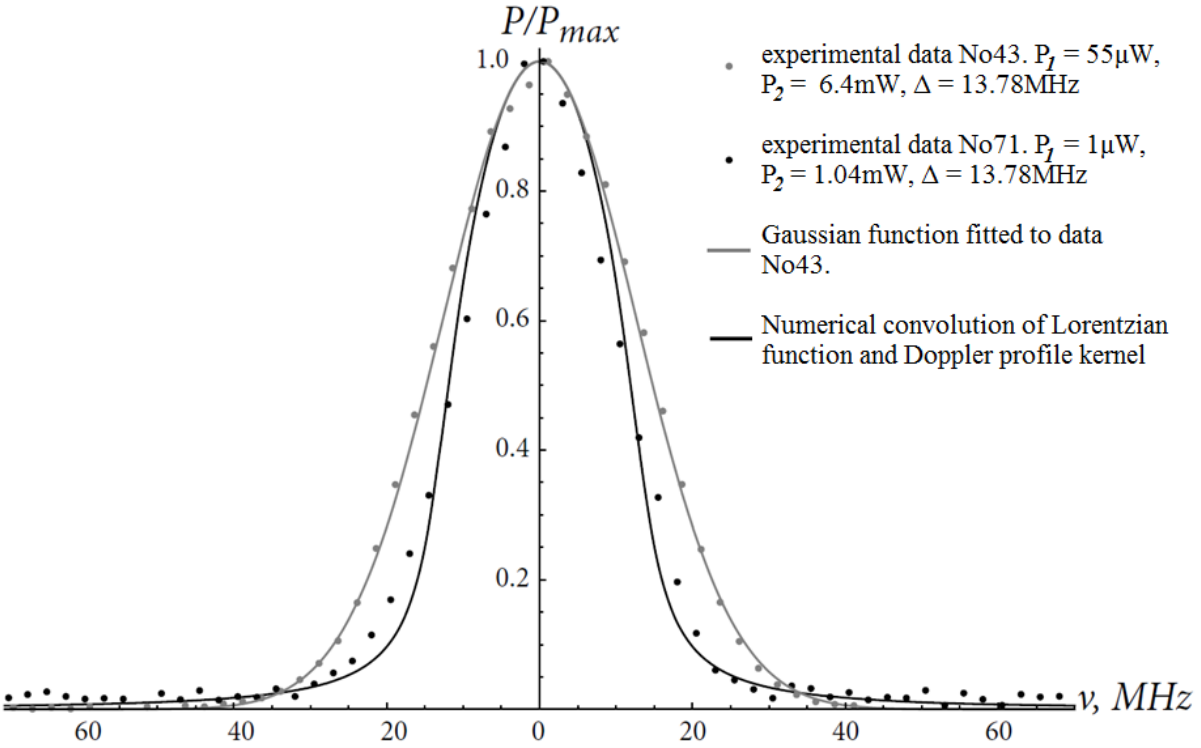

Fig 7. Two normalized measurements of residual Doppler profiles in atomic transition $3S_{1/2} \rightarrow 3P_{1/2} \rightarrow 7D_{3/2}$ in sodium.

2. Hyperfine structure of laser-dressed atomic states

Interaction between electronic cloud of an atom and multipole magnetic and electric fields created by nucleus of the atom leads to splitting of atomic fine structure energy levels into hyperfine structure. The interaction is commonly known as the hyperfine interaction. The hyperfine splitting of atomic ground state and first excited states is usually large enough to address individual hyperfine structure levels by means of spectroscopy. However, in experiments involving manipulation of highly excited atomic states it is impossible to address individual hyperfine levels, and hyperfine structure of the states involved in the experiment must be taken into account. Effect of hyperfine interaction becomes particularly important in level crossing experiments which involve interference of electronic wavefunctions. A theory describing formation of hyperfine structure of dressed states was developed within the research project.

A good example is the method for high efficiency coherent population switching between quantum states developed at the Laser Centre [N. N. Bezuglov, R. Garcia-Fernandez, A. Ekers, K. Miculis, L. P. Yatsenko, K. Bergmann, Phys. Rev. A 78, 053804 (2008)]. Suggested method describes how using the Autler-Townes effect one can create a Landau-Zener interferomenter of atomic energy levels (fig 8).

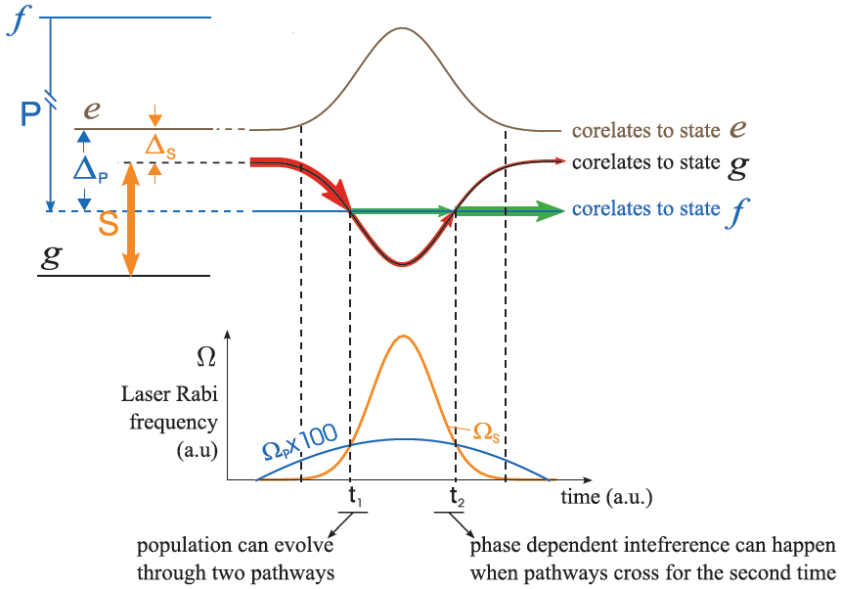

Fig 8. A schematic representation of the method for coherent population switching of a highly excited quantum state. Populations of levels ***g*** and ***f*** at the end of the experiment are determined by the result of interference of the two corresponding wavefunctions at the second crossing point at t_2.

Correct evaluation of hyperfine structure effect on evolution of the laser-dressed states are critical to understanding formation of interference and controlling its contrast. While evaluation of hyperfine splitting of so-called bare atomic states is a standard procedure, effect of hyperfine interaction on laser-dressed atomic state structure had not been investigated theoretically. Strong interaction between an atom and a laser field introduces significant changes in electronic configuration of the atom which may lead to the hyperfine structure of laser-dressed states being qualitatively different from hyperfine structure of bare atomic states. Therefore an analytical theoretical model was created to describe the formation of the hyperfine structure of laser-dressed atomic states.

Time evolution of a wavefunction describing an isolated atomic system is governed by the stationary Schrodinger equation. An atom can be viewed as a system consisting of two interacting parts: nucleus and electronic cloud residing in a Coulomb potential well of the atomic nucleus. The Hamiltonian $\hat{H}_0$ of such system consists of electronic part $\hat{H}_{el}$, nuclear part $\hat{H}_N$ and hyperfine interaction part $\hat{V}_{hf}$. Conventional laser spectroscopy does not involve manipulation of state of atomic nucleus, therefore $\hat{H}_N$ is usually neglected in calculations. Eigenstates of the electronic Hamiltonian $\hat{H}_{el}$ are atomic fine structure states $\left|\zeta, m_J\right\rangle$, energies of which are E_ζ. Here ζ represents a collection of all quantum numbers relevant to the fine structure state and m_ζ is the secondary total electronic angular momentum quantum number. Hyperfine interaction Hamiltonian $\hat{V}_{hf}$ describes interaction between the electronic cloud and electric and magnetic multipole fields created by the atomic nucleus. Usually it is enough to take into account only the magnetic dipole and electric quadrupole interactions $\hat{V}_{dd}$ and $\hat{V}_{qq}$ interactions according to:

$$\hat{V}_{dd} = \hat{A}\hat{\boldsymbol{I}}\cdot\hat{\boldsymbol{J}}$$

$$\hat{V}_{qq} = \hat{B}\,\frac{3\left(\hat{\boldsymbol{I}}\cdot\hat{\boldsymbol{J}}\right)^2 + \frac{3}{2}\hat{\boldsymbol{I}}\cdot\hat{\boldsymbol{J}} - \hat{\boldsymbol{I}}^2\hat{\boldsymbol{J}}^2}{2I(2I-1)J(2J-1)}$$

Here $\hat{\boldsymbol{I}}$ is the nuclear spin vector-operator and $\hat{\boldsymbol{J}}$ is the total electronic angular momentum vector-operator, and *I* and *J* are their corresponding quantum numbers. Operators $\hat{A}$ and $\hat{B}$ commute with the electronic Hamiltonian $\hat{H}_{el}$ and their eigenvalues are the magnetic dipole and electric quadrupole constants for each fine structure state. Spectroscopic measurements do not change the value of nuclear spin *I*, therefore state of the atomic nucleus is completely described by the secondary nuclear spin quantum number m_I. The total atomic wavefunction can be then described using eigenstate basis of the operators $\hat{\boldsymbol{I}}$ and $\hat{\boldsymbol{J}}$. The corresponding ket-vectors are $\left|\zeta, m_J, m_I\right\rangle$. Usually the basis of the total atomic angular momentum vector-operator $\hat{\boldsymbol{F}} = \hat{\boldsymbol{J}} + \hat{\boldsymbol{I}}$ eigenstates is used to diagonalize the total Hamiltonan $\hat{H}_0$. However the standard approach can be used only in the case when all external interactions are much weaker than the weakest internal interaction taken into account when calculating $\hat{H}_0$.

Components of a quantum mechanical angular momentum operator $\hat{\boldsymbol{L}}$ are usually expressed using the so-called spherical basis, $\hat{\boldsymbol{L}} = \left\{L^{-1}, L^0, L^1\right\}$. Each component of the operator influences eigenstate $\left|l, m_l\right\rangle$ of $\hat{\boldsymbol{L}}$ in the following way:

$$\hat{\boldsymbol{L}}^2\left|l, m_l\right\rangle = l(l+1)\left|l, m_l\right\rangle$$

$$L^0\left|l, m_l\right\rangle = m_l\left|l, m_l\right\rangle$$

$$L^{\pm1}\left|l, m_l\right\rangle = \sqrt{l(l+1) - m_l(m_l \mp 1)}\left|l, m_l \mp 1\right\rangle$$

Lasers are an excellent source of coherent and monochromatic electromagnetic field. In the semiclassical picture, a laser beam is usually modeled as a harmonic wave,

$$\boldsymbol{E}(\boldsymbol{r},t) = E_0 \cdot \mathrm{Re}\left(\boldsymbol{\varepsilon} \cdot e^{i(\boldsymbol{k}\cdot\boldsymbol{r}-\omega t)}\right),$$

Here E_0 is amplitude of electric field, ε is a complex polarization vector, $\boldsymbol{k}$ is the wave vector, and ω is angular frequency of the laser beam. At presence of such harmonic perturbation, an atomic system undergoes a transition between energy eigenstates, if the frequency of the perturbation coincides with resonance frequency of the atomic transition. An isolated atom which resides in an energy eigenstate is an electrically neutral particle. However, in transition between eigenstates atom possesses electric and magnetic multipole momenta. For an electric dipole transition all higher multipole effects are usually negligible and interaction Hamiltonian is modeled as interaction between an electric dipole and the electric field. In addition, atomic systems ($\sim 10^{-11}\,m$) are small compared to typical wavelength range of lasers ($\sim 10^{-7}\,m$). Therefore spatial dependence of the laser field is usually neglected. The corresponding expression for the interaction Hamiltonian is then:

$$\hat{V} = E_0 \cdot \mathrm{Re}\left(\hat{\boldsymbol{d}} \cdot \boldsymbol{\varepsilon} \cdot e^{-i\omega t}\right).$$

Here $\hat{\boldsymbol{d}} = -|e|\hat{\boldsymbol{r}}$ is vector-operator for electric dipole moment induced by the laser. In general, time evolution of periodically perturbed system is governed by the time-dependent Schrodinger equation,

$$-i\frac{\partial \Psi}{\partial t} = \hat{H}\Psi.$$

Here Ψ is the wavefunction of the system and eigenvalues of the total Hamiltonian $\hat{H} = \hat{H}_0 + \hat{V}$ are measured in units of angular frequency. If interaction time between a quantum system and an external field is much larger than oscillation period of the field, time-dependent terms in the Hamiltonian can be eliminated via the Rotating wave approximation (RWA). In geometrically cooled supersonic atomic beams a typical atom-laser beam interaction time is $10^{-7}\,s$ and oscillation period of visible light is $10^{-12}\,s$. Therefore the RWA is applicable. Application of the RWA involves specific choice of basis vectors $|\varphi\rangle$ which are related to the stationary eigenstates $|\varphi_0\rangle$ of $\hat{H}_0$ via a specific unitary transformation $\hat{U}$. The total Hamiltonian of the system is transformed in the following way:

$$\tilde{\hat{H}} = \hat{U}^{-1}\hat{H}\hat{U} - i\hat{U}^{-1}\frac{\partial \hat{U}}{\partial t}.$$

In the rotating wave approximation diagonal elements of the Hamiltonian represent laser detuning $\Delta = \omega - \omega_0$ from resonance frequency ω_0 of transition between states $|g\rangle$ and $|e\rangle$. Off-diagonal elements corresponding to atom – laser field interaction contain halved time-independent Rabi frequencies $\Omega_{ge} = \frac{\langle e|\hat{\boldsymbol{d}} \cdot \boldsymbol{E}_0|g\rangle}{\hbar}$. Interestingly, time-independent interaction Hamiltonians not connecting different energy levels (like the hyperfine interaction Hamiltonian) are not affected by the transformation. Eigenvalue spectrum and eigenstates of the stationary RWA Hamiltonian are obtained by solving the stationary Schrodinger equation.

Eigenstates of the semiclassical system atom + laser field are called dressed states contrary to the states of isolated atom, which are usually referred to as bare states. The dressed state approach is conventionally used to describe systems which can be modeled as collections of independent two-state systems or collection of independent

multilevel ladder excitation schemes. Presence of the hyperfine interactions renders such approximation impossible as the interaction couples several sublevels of each energy level. To overcome this difficulty the basis of the total atomic angular momentum $\hat{F}$ is commonly used since in this basis Hamiltonian of an isolated atom is already diagonal. At presence of a strong external perturbation $\hat{F}$ does not provide a set of good quantum numbers. Therefore the conventional approach is not applicable. Mathematical description of dressed states was adapted to describe eigenstates in the case of non-diagonal Hamiltonian $\hat{H}_0$. Consider a system consisting of two fine structure levels $\zeta = g, e$, each level being composed of $2J_\zeta + 1$ sublevels $\left|\zeta, m_\zeta\right\rangle$. Each dressed state of the system is identified using set of two quantum numbers $s = \pm 1$ and m. The following expression relates bare and dressed states:

$$\left|\Phi_{s,m}\right\rangle = \cos\theta_{s,m}\left|g, m_g\right\rangle + \sin\theta_{s,m}\left|e, m_g + p\right\rangle$$

$$E_{s,m} = \frac{1}{2}\left(\Delta + s\sqrt{\Delta^2 + \Omega_m^2}\right)$$

Here p describes polarization of the laser field with $p = \pm 1$ corresponding to circular $\sigma^\pm$ polarization while $p=0$ corresponds to linear π polarization. Mixing angle $\theta_{s,m}$ is defined as:

$$\tan\theta_{s,m} \equiv \frac{\Omega_m}{E_s},$$

Rabi frequency Ω_m corresponds to rabi frequency of transition $\left|g, m_g\right\rangle \leftrightarrow \left|e, m_g + p\right\rangle$. Elliptically polarized laser field induces transitions from a single ground state $\left|g, m_g\right\rangle$ to multiple excited states $\left|e, m_e\right\rangle$, and in this case it is necessary to choose a specific set of stationary basis vectors described in 1983 paper by J.R. Morris and B. W. Shore [J. R. Morris and B. W. Shore, Phys. Rev. A 27, 906-912 (1983)]. Theoretical description of a quantum system becomes very complicated in this case. Therefore only $p = 0, \pm 1$ were considered in this study.

In general, all quantum states, even dark states, of the system must be taken into account. However, in the case of very strong external perturbation overall influence of the dark states is negligible and dark states can be safely discarded from the description. However it is now very important to identify quantum numbers m_g corresponding to bright states and to define exact relation between quantum numbers m and m_g to be used in relation between $\left|\Phi_{s,m}\right\rangle$ and $\left|g, m_g\right\rangle, \left|e, m_g + p\right\rangle$:

- If J_g is a half-integer, $m_g \in \left[-J_g + \alpha(-1); J_g - \alpha(1)\right]$,
- If J_g is an integer, $m_g \in \left[-J_g + \alpha(-1); 0\right) \cup \left(0; J_g - \alpha(1)\right]$,

$$\alpha(x) = \frac{1}{2}(p + x)(1 - \Delta J)(p \cdot \Delta J + p - x \cdot \Delta J)$$

Here $\Delta J = J_e - J_g$. A convenient way to relate the quantum numbers m and m_g is to define $m \equiv m_g$ for values of m_g satisfying the above conditions.

In the dressed atomic state energy level diagram three regions corresponding to different proportions between hyperfine and atom-laser interaction energies (fig 9.):

1) Hyperfine structure interaction dominates over atom – laser field interaction;
2) Both interaction energies are approximately equal;

3) Atom – laser dominates over hyperfine structure interaction.

In the first case hyperfine splittings of ground and excited state are large enough to address individual hyperfine structure levels. All other quantum states remain unaffected by atom – laser field interaction. Eigenstates of the system are well described by the conventional dressed state approach, and in this case a finer structure of Autler-Townes doublets is not observed.

In the second case, strong interaction between all quantum states of the system is present, and analytical solutions for an arbitrary atomic system do not exist. Analytical solutions may be obtained for specific quantum systems only. Numerical methods for determining energies and populations of quantum states are most effective if large numbers of quantum states are involved.

In the third case atom- laser field interaction results in formation of dressed states which are split into hyperfine structure. Due to large splitting between dressed states, analysis of the system using first order perturbation theory allows several approximations which introduce significant simplifications in the theoretical description of the system. In this case it is possible to obtain analytical expressions for the energy level spectrum in general case. A theory describing formation of hyperfine structure of dressed states was developed within the research project.

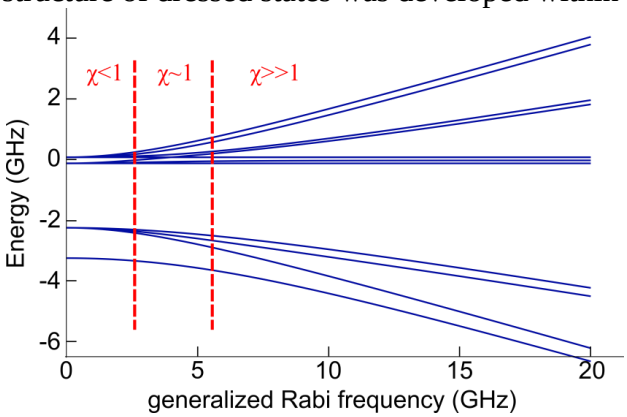

Fig 9. Quantum state energy diagram for atomic system *I=1/2*, J_g*=1/2*, J_e*=3/2*, A_g*=1GHz*, A_e*=0.1GHz*. The three regions correspond to different values of the ratio χ between external interaction strength and hyperfine interaction strength.

Investigation of hyperfine structure of dressed states requires all matrix elements of $\hat{V}_{hf}$ to be calculated in the dressed state basis,

$$\left\langle \Phi_{s,m}, m_I \left| \hat{V}_{hf} \right| \Phi_{s',m'}, m'_I \right\rangle = \cos\theta_{s,m} \cos\theta_{s',m'} \left\langle g, m, m_I \left| \hat{V}_{hf} \right| g, m', m'_I \right\rangle +$$
$$+ \sin\theta_{s,m} \sin\theta_{s',m'} \left\langle e, m+p, m_I \left| \hat{V}_{hf} \right| e, m'+p, m'_I \right\rangle$$

The first order perturbation approach allows interaction between nondegenerate quantum states to be neglected. Therefore all possible degeneracies in the dressed state picture must be investigated. Energy spectra of dressed states is composed of two nondegenerate branches, s=+1 and $s=-1$, split apart by $\Delta E = \sqrt{\Delta^2 + \Omega_m^2}$. Dressed states are degenerate only by sign of corresponding Rabi frequency since energies of the dressed states depend on absolute value of the Rabi frequency. Therefore conditions for all cases when $\Omega_m^2 = \Omega_{m'}^2$ must be identified. Symmetry properties of both quantum system and laser radiation suggest that such degeneracies only occur if $p \cdot \Delta J = 0$. In this case dressed states $\left|\Phi_{s,m}\right\rangle$ and $\left|\Phi_{s,-m-p}\right\rangle$ are

degenerate. In all other cases dressed states $\left|\Phi_{s,m}\right\rangle$ are nondegenerate. Degeneracy by nuclear spin secondary quantum number m_I arises from the fact that atom – laser field interaction does not alter state of nucleus. Therefore all quantum states of the full system $\left|\Phi_{s,m},m_I\right\rangle$ are $(2I+1)$–times degenerate. According to this analysis, up to the first order it is sufficient to take into account only elements $\left\langle\Phi_{s,m},m_I\left|\hat{V}_{hf}\right|\Phi_{s,m},m_I'\right\rangle$ of the hyperfine Hamiltonian matrix. In the case of $p\cdot\Delta J=0$ additional elements $\left\langle\Phi_{s,m},m_I\left|\hat{V}_{hf}\right|\Phi_{s,-m-p},m_I'\right\rangle$ must be taken into account. To avoid lengthy and incomprehensible expressions it is convenient to calculate effects of magnetic dipole part $\hat{V}_{dd}$ and electric quadrupole part $\hat{V}_{qq}$ of hyperfine Hamiltonian separately.

Matrix elements of the magnetic dipole operator $\hat{V}_{dd}$ are easily obtained by expanding the operator in the spherical basis, $\hat{V}_{dd}=\hat{A}\hat{\boldsymbol{I}}\cdot\hat{\boldsymbol{J}}=\hat{A}\left(\hat{I}^0\hat{J}^0-\hat{I}^1\hat{J}^{-1}-\hat{I}^{-1}\hat{J}^1\right)$. Analysis of structure of the matrix element

$$\left\langle\Phi_{s,m},m_I\left|\hat{V}_{dd}\right|\Phi_{s,m},m_I'\right\rangle=\left\langle\Phi_{s,m},m_I\left|\hat{A}\left(\hat{I}^0\hat{J}^0-\hat{I}^1\hat{J}^{-1}-\hat{I}^{-1}\hat{J}^1\right)\right|\Phi_{s,m},m_I'\right\rangle$$

shows that the only term giving nonzero contribution to the matrix element is $\hat{A}\hat{I}^0\hat{J}^0$. The resulting matrix for $\hat{V}_{dd}$ in the case of $p\cdot\Delta J\neq 0$ is diagonal to the first order in the dressed state basis. Magnetic dipole interaction between electronic cloud and nucleus results in lifting of degeneracy by m_I,

$$\begin{aligned}\left\langle\Phi_{s,m},m_I\left|\hat{V}_{dd}\right|\Phi_{s,m},m_I'\right\rangle&=A_g\cos^2\theta_{s,m}\left\langle g,m,m_I\left|\left(\hat{I}^0\hat{J}^0-\hat{I}^1\hat{J}^{-1}-\hat{I}^{-1}\hat{J}^1\right)\right|g,m,m_I'\right\rangle+\\&+A_e\sin^2\theta_{s,m}\left\langle e,m+p,m_I\left|\left(\hat{I}^0\hat{J}^0-\hat{I}^1\hat{J}^{-1}-\hat{I}^{-1}\hat{J}^1\right)\right|e,m+p,m_I'\right\rangle=\\&=m_I\delta_{m_I,m_I'}\left[A_g m\cos^2\theta_{s,m}+A_e(m+p)\sin^2\theta_{s,m}\right]\end{aligned}$$

Off-diagonal terms significant when $p\cdot\Delta J=0$ are given by the following expression:

$$\left\langle\Phi_{s,m},m_I\left|\hat{V}_{dd}\right|\Phi_{s,-m-p},m_I'\right\rangle=\frac{\delta_{m_I'\pm1,m_I}\delta_{m,\mp\frac{1\pm p}{2}}}{2}\sqrt{I(I+1)-m_Im_I'}\cdot$$

$$\cdot\left(A_g\sqrt{J_g(J_g+1)+\frac{(1+p)(1-p)}{4}}\cos^2\theta_{s,m}+A_e\sqrt{J_e(J_e+1)+\frac{(1+p)(1-p)}{4}}\sin^2\theta_{s,m}\right)$$

Analysis of the off-diagonal terms of Hamiltonian $\hat{V}_{dd}$ shows that only two pairs of dressed states $\left|\Phi_{s,m},m_I\right\rangle$ are coupled together by this interaction. In addition no off-diagonal elements are present if the following conditions are not satisfied:

a) In the case of linear polarization (*p=0*), if the total electronic angular momentum quantum numbers of ground and excited state J_g and J_e are half-integers, then the dipole interaction couples quantum states $\left\{\left|\Phi_{s,\frac{1}{2}},m_I\right\rangle,\left|\Phi_{s,-\frac{1}{2}},m_I+1\right\rangle\right\}$;

b) In the case of circular polarization ($p=\pm1$), if the total electronic angular momentum quantum numbers of ground and excited state J_g=J_e are integers,

then the dipole interaction couples dressed states $\left\{\left|\Phi_{s,\frac{1-p}{2},m_I}\right\rangle,\left|\Phi_{s,-\frac{1+p}{2},m_I+1}\right\rangle\right\}$.

Analysis of the electric quadrupole interaction Hamiltonian $\hat{V}_{qq}$ yields similar results. The only nonzero term of the matrix element $\left\langle\Phi_{s,m},m_I\left|\hat{V}_{qq}\right|\Phi_{s,m},m_I'\right\rangle$ is given by an operator which again gives no off-diagonal terms:

$$\hat{B}\frac{3\left(\hat{I}^q\hat{I}^{-q}\hat{J}^{-q}\hat{J}^q\right)+\frac{3}{2}\hat{I}^0\hat{J}^0-\hat{\boldsymbol{I}}^2\hat{\boldsymbol{J}}^2}{2I(2I-1)J_\zeta(2J_\zeta-1)}$$

Additional energy shift arising from the quadrupole interaction can be expressed as:

$$\left\langle\Phi_{s,m},m_I\left|\hat{V}_{qq}\right|\Phi_{s,m},m_I'\right\rangle=\delta_{m_I,m_I'}\frac{I(I+1)-3m_I^2}{4I(2I-1)}\cdot\left(B_g\frac{J_g(J_g+1)-3m^2}{J_g(2J_g-1)}\cos^2\theta_{s,m}+\right.$$

$$\left.+B_e\frac{J_e(J_e+1)-3(m+p)^2}{J_e(2J_e-1)}\sin^2\theta_{s,m}\right)$$

The case when degenerate dressed states are formed at $p\cdot\Delta J=0$ is, however, more complicated than in the dipole interaction case. Nonzero diagonal elements linking states $\left\{\left|\Phi_{s,\frac{1-p}{2},m_I}\right\rangle,\left|\Phi_{s,-\frac{1+p}{2},m_I+1}\right\rangle\right\}$ arise from the operator of form:

$$\hat{B}\frac{-3\left(\hat{I}^1\hat{I}^0\hat{J}^{-1}\hat{J}^0+\hat{I}^0\hat{I}^1\hat{J}^0\hat{J}^{-1}+\hat{I}^0\hat{I}^{-1}\hat{J}^0\hat{J}^1+\hat{I}^{-1}\hat{I}^0\hat{J}^1\hat{J}^0\right)-\frac{3}{2}\left(\hat{I}^1\hat{J}^{-1}+\hat{I}^{-1}\hat{J}^1\right)}{2I(2I-1)J_\zeta(2J_\zeta-1)}$$

And nonzero elements linking dressed states $\left\{\left|\Phi_{s,\frac{2-p}{2},m_I}\right\rangle,\left|\Phi_{s,-\frac{2+p}{2},m_I+2}\right\rangle\right\}$ arise from operator of form:

$$\hat{B}\frac{-3\left(\hat{I}^1\hat{I}^1\hat{J}^{-1}\hat{J}^{-1}+\hat{I}^{-1}\hat{I}^{-1}\hat{J}^1\hat{J}^1\right)}{2I(2I-1)J_\zeta(2J_\zeta-1)}$$

Identical results for all calculations were obtained employing two different methods: operator formalism approach demonstrated above and a different approach, employing Clebsch – Gordan coefficients $C^{L,M}_{l,m,l',m'}$ to transform from eigenvector basis of total atomic angular momentum $\hat{\boldsymbol{F}}$ to the dressed state basis. As mentioned above, the hyperfine structure Hamiltonian is diagonal in $\hat{\boldsymbol{F}}$ eigenstate basis. Energies of each hyperfine component can then be calculated using a simple expression found in most textbooks on atomic structure and spectroscopy,

$$\Delta E(\zeta,F_\zeta)=\frac{1}{2}A_\zeta K_\zeta-B_\zeta\left(\frac{(I+1)(J_\zeta+1)}{2(2I-1)(2J_\zeta-1)}-\frac{2K_\zeta(K_\zeta+1)}{8I(2I-1)J_\zeta(2J_\zeta-1)}\right),$$

here $K_\zeta=F_\zeta(F_\zeta+1)-I(I+1)-J_\zeta(J_\zeta+1)$. Using this approach, expressions containing nontrivial sums of Clebsch – Gordan coefficients are obtained. Numerical calculations have revealed that:

$$\sum_{F=|J-I|}^{J+I}\left(\left[C^{F,m+m_I}_{J,m,I,m_I}\right]^2\left[F(F+1)-I(I+1)-J(J+1)\right]\right)=2m_I m$$

$$\sum_{F=|J-I|}^{J+I}\left(\left[C^{F,m+m_I}_{J,m,I,m_I}\right]^2\left[\frac{(I+1)(J+1)}{2(2I-1)(2J-1)}-\frac{2K(K+1)}{8I(2I-1)J(2J-1)}\right]\right)=$$

$$=\frac{3\left[J(J+1)m_I^2+I(I+1)m^2\right]-9m_I^2m^2-I(I+1)J(J+1)}{2I(2I-1)J(2J-1)}$$

Results of this study have led to conclusion that hyperfine structure of laser-field dressed states differs dramatically from the usual atomic hyperfine structure. In addition, the structure formed depends on choice of laser field polarization (fig 10). Analytical expressions relevant to the case when atom – laser field interaction dominates over hyperfine structure interaction were obtained. The analytical expressions provide a clear physical interpretation for the hyperfine structure of the dressed states: spatial configuration of electronic cloud in a dressed state creates a stationary electric and magnetic fields in which nuclear Zeeman effect and higher multipole analogues of it are observed. A dressed sate creates homogeneous magnetic field which is aligned along the quantization (z) axis,

$$\boldsymbol{B}=B\boldsymbol{e}_z,\ B=-\frac{A_g m\cos^2\theta_{s,m}+A_e(m+p)\sin^2\theta_{s,m}}{\gamma_N},$$

here γ_N is the gyromagnetic ratio of atomic nucleus. The usual nuclear Zeeman effect manifests as splitting of Autler – Townes doublet into *2I+1* components. Energy shift of each component is expressed as:

$$\left\langle m_I\left|\hat{V}_{dd}\right|m_I\right\rangle=\left\langle m_I\left|-\gamma_N\hat{\boldsymbol{I}}\cdot\boldsymbol{B}\right|m_I\right\rangle=m_I\left[A_g m\cos^2\theta_{s,m}+A_e(m+p)\sin^2\theta_{s,m}\right]$$

In addition, the electron cloud in a dressed state creates electric quadrupole field characterized by a tensor, with the only nonzero component Q_{zz},

$$Q_{zz}\propto B_g\frac{J_g(J_g+1)-3m^2}{J_g(2J_g-1)}\cos^2\theta_{s,m}+B_e\frac{J_e(J_e+1)-3(m+p)^2}{J_e(2J_e-1)}\sin^2\theta_{s,m}$$

If nucleus of the atom posesses a nonzero electric quadrupole momentum, additional shifts of hyperfine structure states are observed:

$$\left\langle m_I\left|\hat{V}_{qq}\right|m_I\right\rangle=\frac{I(I+1)-3m_I^2}{4I(2I-1)}\cdot$$

$$\cdot\left(B_g\frac{J_g(J_g+1)-3m^2}{J_g(2J_g-1)}\cos^2\theta_{s,m}+B_e\frac{J_e(J_e+1)-3(m+p)^2}{J_e(2J_e-1)}\sin^2\theta_{s,m}\right)$$

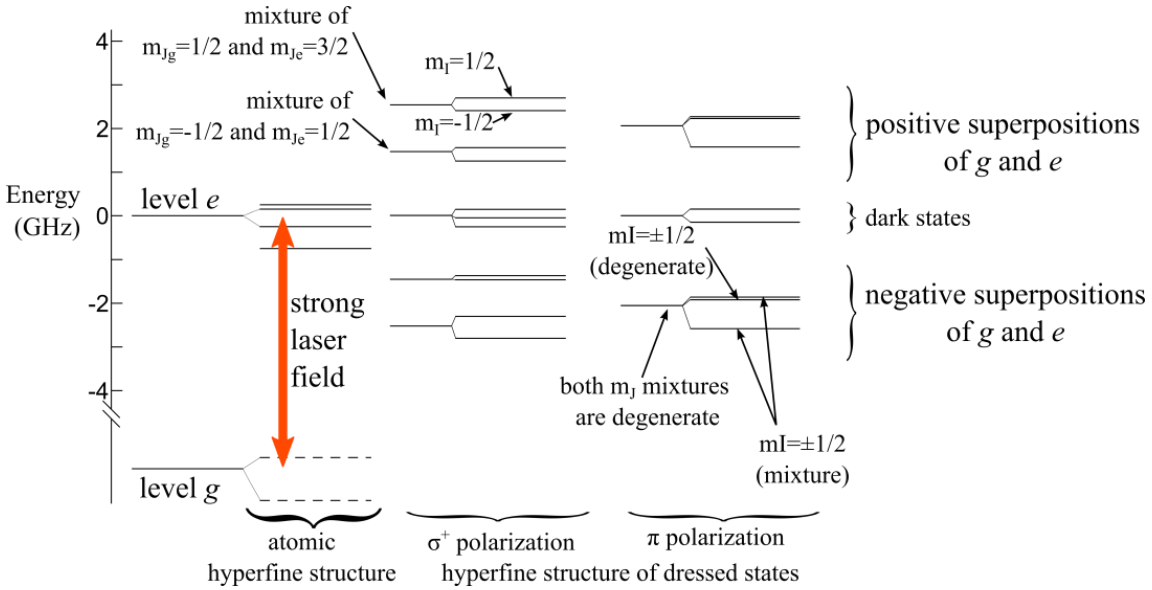

Fig 10. Energy level diagram for an atomic system $I=1/2$, $J_g=1/2$, $J_e=3/2$, $A_g=1GHz$, $A_e=0.2GHz$,$\Omega_0=10GHz$. Hyperfine structure of laser-dressed states differs significantly from hyperfine structure of bare atomic states. In addition, the hyperfine structure can be altered by changing polarization of the pump laser field.

Results of the study were presented at *44th Conference of the European Group on Atomic Systems (EGAS)* in Gothenburg (Sweden) [4] and at the *1st TLL-COLIMA Joint workshop* in Riga [5]. A scientific paper on the subject of the study is being prepared in collaboration with lecturer Dr. V. Kashcheyevs.

3. Measurements of radiative constants of highly excited quantum states

Research topics investigated in Molecular beam laboratory of Laser centre of the University of Latvia include development of new methods for coherent manipulation and population switching of highly excited (Rydberg) quantum states. Optimal choice of excitation scheme is required for experimental realization of these methods. Most important properties of a quantum state are lifetime and branching ratio. Branching ratio characterizes realization probability of different decay channels. In this context new methods which allow evaluation of these parameters to high precision are imperative. Within the research project a new method for measuring radiative constants of highly excited quantum states was developed. The method is based on relation between population dynamics of a state and physically observable properties of emission spectra.

Population dynamics of a quantum system was investigated using the optical Bloch equations for state density matrix:

$$\frac{d\rho}{dt} = -\frac{i}{\hbar}\left[\hat{H}, \rho\right] + R\rho$$

The total Hamiltonian $\hat{H}$ of the system includes both isolated atom Hamiltonian and terms characterizing interaction with external laser fields. Relaxation matrix R represents all incoherent processes taking place in the system. These processes include spontaneous emission and repopulation of quantum states.

Information about population dynamics of a system is contained in the density matrix $\hat{\rho}$. The density matrix of a partially open system is calculated using the optical pumping equations,

$$\dot{\rho}_{nm}(t) = -i\left(\hat{\Omega}\hat{\rho}\right)_{nm} + i\left(\hat{\rho}\hat{\Omega}\right) - \hat{\Gamma}\hat{\rho}$$

Here ρ_{ij} are elements of the density matrix, matrix $\hat{\Omega}$ contains Rabi frequencies which characterize atom – laser field interaction strength, and matrix $\hat{\Gamma}$ accounts for spontaneous emission. Konstantinov – Perel diagram method assigns a graphical representation to each process taking place in the system (fig 11), thus simplifying analysis of the optical Bloch equations for multilevel systems.

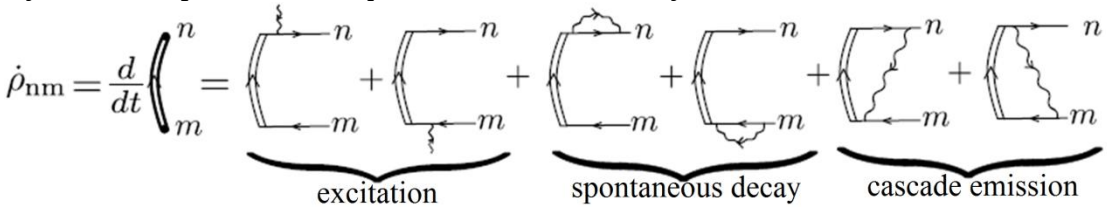

Fig 11. An optical pumping rate equation using the Konstantinov-Perel diagrams.

Expression relating lifetime $1/\Gamma_f$ of a highly excited state and ratio $\rho_f^{(area)}$ of relative intensities of Autler – Townes doublet components were obtained after careful analysis of the pumping rate equations in the adiabatic approximation,

$$\rho_f^{(area)} = \frac{\int_{-\infty}^{\infty} d\Delta_{10}\, I_f^{(1)}(\Delta_{10})}{\int_{-\infty}^{\infty} d\Delta_{20}\, I_f^{(2)}(\Delta_{20})} = \frac{\Gamma_{t2}}{\Gamma_{t1}} = \frac{(\Gamma_{ef} + \Gamma_f)\sin^2\theta + \Gamma_e \cos^2\theta}{(\Gamma_{ef} + \Gamma_f)\cos^2\theta + \Gamma_e \sin^2\theta}$$

Here Θ is the mixing angle which relates each dressed state to two bare states. Numerical simulations were performed using excitation scheme $3S_{1/2} \rightarrow 3P_{1/2} \rightarrow Rydberg$ in sodium atoms (fig 12). Rabi frequencies of the transitions were assumed to be accordingly 10MHz and 100MHz.

The theoretical model developed in this study predicts that relation between lifetime ratio and ratio of spectral lineshape areas becomes linear at large values of detuning Δ from transition resonance frequency (fig 12). Numerical simulations employing ladder excitation scheme $3S_{1/2} \rightarrow 3P_{1/2} \rightarrow 7D_{3/2}$ in sodium were performed to test practical usability of the method. Optical Bloch equations were solved for a partially open three level system employing the Konstantinov – Perel diagram technique. Results of the simulation have revealed that the linear dependence is observed at detunings $\Delta > 70\ MHz$ from resonance of the transition $3P_{1/2} \rightarrow 7D_{3/2}$. In this case intensity of the two-photon transition is well below experimental noise level (fig 13) and cannot be measured using equipment available at the Laser centre. Rapid decrease in intensity of the two-photon peak is linked to the large lifetime difference of states $3P_{1/2}$ and $7D_{3/2}$. Lifetimes of the levels are accordingly *16.29ns* and *305ns*. Verification of the mathematical model requires choice of states with less different lifetimes. However such experimental measurements could not be performed currently due to limitations of experimental capacity of the laboratory.

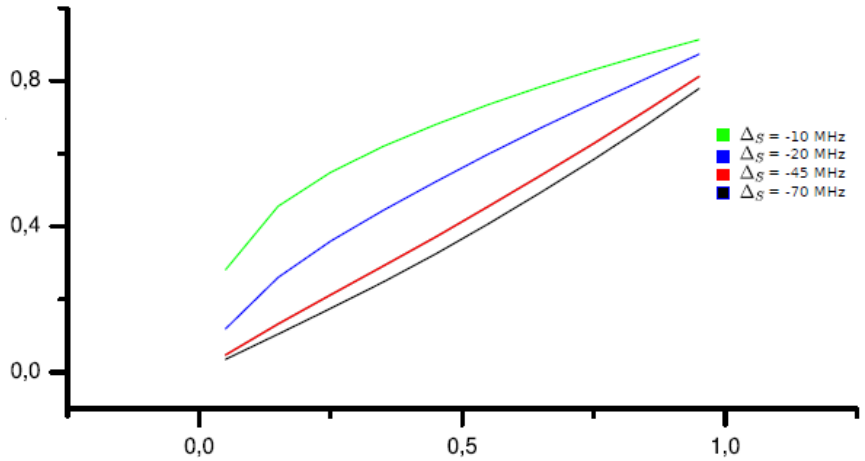

Fig 12. Relative are ratio $\rho_f^{(area)}$ of Autler-Townes doublet components as a function of ratio τ_e / τ_f between lifetimes of two corresponding bare states *e* and *f*. Here $\tau_e = 16.23\ ns$. Detuning of the strong pump laser is represented by Δs.

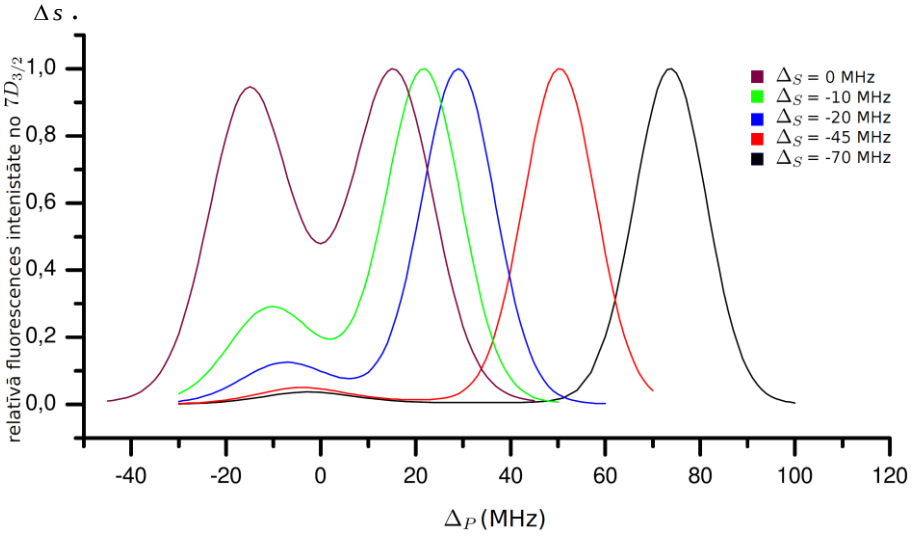

Fig 13. Relative intensities of Autler-Townes doublet components at different detunings from resonance frequency of transition $3P_{1/2} \rightarrow 7D_{3/2}$ in sodium.

Results of the study were compiled in bachelor thesis "*Atomu izstarošanas konstanšu mērījumi virsskaņas nātrija atomu kūlī, izmantojot nepārtrauktu lāzera ierosmi*" ("Measurements of radiative constants in sodium supersonic atomic beam using continuous wave laser excitation") by S. Mezinska. The method for lifetime measurements of highly excited atomic states was presented at conference *Developments in Optics and Communications 2011* (Riga) [6].

4. Technological improvements to experimental capacity of the Molecular beam laboratory.

Regular maintenance and improvement of laboratory devices was carried out to maintain and improve quality and potential of experimental scientific studies at Molecular beam laboratory of Laser Centre of the University of Latvia. There are three main components for every experimental setup: laser system, main experimental device (e.g. molecular beam machine) and devices which collect experimental data.

Experimental studies can be conducted successfully only if excellent simultaneous operation of these components is achieved.

The molecular beam machine contains large amount of highly chemically active sodium. Therefore low atmospheric pressure ($\sim 10^{-2}\,Torr$) must be maintained continuously inside the machine.

High precision laser spectroscopy requires excellent operation of the laser system. Internal frequency stabilization electronics are effective only for avoiding mode hops and are ineffective when long-term frequency stabilization is required. Atomic and molecular systems are used as frequency standards worldwide and therefore can be used for laser frequency long term stabilization. Usually a wavelength meter is employed for continuous frequency control. As a part of the research project, a system for long term absolute laser frequency stabilization was developed by using saturated absorption spectroscopy methods in sodium vapor cell [fig_14].

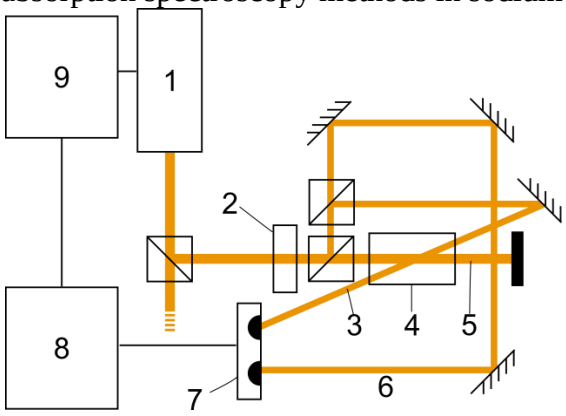

Fig 14. Laser frequency stabilization using saturated absorption in sodium vapour cell. 1 – the laser; 2 – acousto-optic modulator, 3 – probe beam, 4 – sodium vapour cell, 5 – saturating beam, 6 – reference beam, 7 – differential amplifier, 8 – signal processing unit, 9 – laser frequency controller.

The saturating beam ensures that absorption profile for probe beam is without Doppler broadening and formation of Lamb dips can occur. Therefore frequency of the laser beam can be fine-tuned to a specific atomic/molecular transition. Differential amplifier is used to measure very small variations in laser beam absorption. Acousto-optic modulator in conjunction with lock-in amplifier ensures that the signal sent to the signal processing unit corresponds to first derivative of saturated absorption spectrum. Therefore even higher sensitivity to small variations of frequency is achieved.

Accuracy of frequency stabilization scheme using a wavelength meter depends on calibration of the device and other device parameters. The system developed provides excellent precision which does not decay over time. In addition, the stabilization scheme is compatible with cells containing many kinds of atomic/molecular vapors.

Conferences theses

[1] **M. Bruvelis, A. Cinins, S. Mezinska, N. N. Bezuglov, I. I. Ryabtsev and A. Ekers**, *Particularities of Doppler profile for supersonic beams with circular, square, and arbitrary collimating apertures*, 43rd Conference of the European Group for Atomic Systems (EGAS), University of Fribourg, Fribourg, Switzerland, June 28 – July 2 2011;

[2] **M. Bruvelis, N. N. bezuglov and A. Ekers**, Doppler Profile Particularities in Supersonic Beams for Circular, Square and Arbitrary Collimating Apertures, 21st International Conference on Spectral Line Shapes, St. Petersburg, Russia, June 3–9, 2012.

[3] **M. Bruvelis, A. Cinins, S. Mezinska, K. Miculis, N. N. Bezuglov and A. Ekers**, *Particularities of Doppler profile for supersonic beams with circular, square, and arbitrary collimating apertures*, nepublicēts raksts.

[4] **A. Cininsh and V. Kashcheyevs**, Hyperfine structure of laser-dressed atomic states, 44th Conference of the European Group on Atomic Systems (EGAS) Gothenburg, Sweden, July 9-13, 2012

[5] **A. Cininsh and V. Kashcheyevs**, Hyperfine structure of laser-dressed atomic states, 1st TLL-COLIMA Joint workshop, Riga, Latvia, July 18-19, 2012

[6] **S. Mezinska, M. Bruvelis, V. Kashcheyevs**, Measurements of radiative constants in sodium supersonic atomic beam using continuous wave laser excitation, Developments in Optics and Communications 2011, Riga, Latvia, April 28-30, 2011

[7] **M. Bruvelis, J. Ulmanis, K. Miculis, N. N. Bezuglov, C. Andreeva, and A. Ekers** "Interference patterns of laser-dressed states in a supersonic atomic/molecular beam", Frotniers of Matter Wave Optics FOMO 2011, Obergurgl, Austrija, March 20-25, 2011

Doctoral school seminars

[8] **Mārtiņš Brūvelis**, Residual Doppler Profile in Supersonic Molecular Beam, Latvijas Universitātes Doktorantūras skolas „Atomāro un nepārtrauktās vides fizikālo procesu pētīšanas, modelēšanas un matemātisko metožu pilnveidošanas skola" seminārs, Rīga, 10. novembris, 2010

[9] **Mārtiņš Brūvelis**, Spatial control of Na excitation by means of interference due to Autler-Townes effect, Latvijas Universitātes Doktorantūras skolas „Atomāro un nepārtrauktās vides fizikālo procesu pētīšanas, modelēšanas un matemātisko metožu pilnveidošanas skola" seminārs, Rīga, 16. februāris, 2011

[10] **Artūrs Ciniņš**, Hyperfine splitting of atomic levels in strong laser field limit, Latvijas Universitātes Doktorantūras skolas „Atomāro un nepārtrauktās vides fizikālo procesu pētīšanas, modelēšanas un matemātisko metožu pilnveidošanas skola" seminārs, Rīga, 22. februāris, 2012